Atmos. Meas. Tech. Discuss., 2, 2983–3025, 2009
www.atmos-meas-tech-discuss.net/2/2983/2009/

Atmospheric Measurement Techniques Discussions

This discussion paper is/has been under review for the journal Atmospheric Measurement Techniques (AMT). Please refer to the corresponding final paper in AMT if available.

Retrieval of tropospheric column densities of NO_2 from combined SCIAMACHY nadir/limb measurements

S. Beirle, S. Kühl, J. Puķīte, and T. Wagner

Max-Planck-Institut für Chemie, Mainz, Germany

Received: 6 November 2009 – Accepted: 11 November 2009 – Published: 23 November 2009

Correspondence to: S. Beirle (steffen.beirle@mpic.de)

Published by Copernicus Publications on behalf of the European Geosciences Union.

Abstract

The SCIAMACHY instrument onboard the ESA satellite ENVISAT allows the retrieval of column densities of various trace gases, among them NO_2. As only instrument of its kind, SCIAMACHY measures in an alternating limb/nadir mode. The limb measurements allow a direct determination of stratospheric column densities, which are needed to extract tropospheric from the total column density measurements performed in (quasi simultaneous) nadir geometry.

Here we discuss the potential and limitations of SCIAMACHY limb measurements for estimating stratospheric column densities of NO_2 in comparison to a simple reference sector method, and the consequences for the resulting tropospheric column densities. A direct, absolute limb correction scheme improves spatial patterns of tropospheric NO_2 column densities at high latitudes compared to the simple reference sector method. However, it results in artificial zonal stripes at low latitudes. Thus, also a *relative* limb correction scheme was defined, which turned out to successfully reduce stratospheric artefacts in the resulting tropospheric data product without introducing new ones. This relative limb correction scheme is rather simple, robust, and, in essence, based on measurements alone.

The effect of the different stratospheric estimation schemes on tropospheric column densities is discussed with respect to zonal and temporal dependencies. In addition, error quantities are defined from the nadir/limb measurements which indicate remaining systematic errors as function of latitude and day.

Our new suggested stratospheric estimation scheme, the relative limb correction, improves monthly mean tropospheric slant column densities significantly, e.g. from -1×10^{15} molec/cm^2 (using a simple reference sector method) to ≈ 0 in the Atlantic ocean, and from $+1 \times 10^{15}$ molec/cm^2 to ≈ 0 over Siberia, at 50° N in January.

AMTD

2, 2983–3025, 2009

1 Introduction

Satellite-borne UV-vis spectrometers, like the Global Ozone Monitoring Experiment (GOME 1 & 2), the SCanning Imaging Absorption Spectrometer for Atmospheric CHartographY (SCIAMACHY), or the Ozone Monitoring Instrument (OMI) (e.g. Burrows et al., 1999; Bovensmann et al., 1999; Levelt et al., 2006), which have originally been designed for monitoring stratospheric ozone, allow also the retrieval of various additional atmospheric trace gases like NO_2, SO_2, H_2O, OClO, BrO, IO, HCHO, or Glyoxal, on global scale (e.g. Burrows et al., 1999; Martin et al., 2008; Wagner et al., 2008). In particular the retrieval of tropospheric NO_2 column densities has been demonstrated and analyzed in several studies with numerous scientific applications over the last years (see for instance Martin et al., 2008, and references therein).

From the spectrally resolved nadir measurements, total slant column densities (SCDs), i.e. concentrations integrated along the effective light path, can be derived by differential optical absorption spectroscopy (DOAS) (Platt and Stutz, 2008) or similar techniques. SCDs can be transformed to vertical column densities (VCDs) by accounting for radiative transfer in the atmosphere. Note that in the following we use the inspecific term "column densities" (CDs), but define and discuss the matter of vertical versus slant column densities in detail in Sect. 2.4 and 2.5.

If one is interested in tropospheric CDs of trace gases that are present both in stratosphere and troposphere, the stratospheric fraction has to be removed from the total atmospheric CDs. This is a particularly challenging task in the case of O_3, since the bulk of the total CD is located in the stratosphere. Different methods estimate stratospheric ozone CDs e.g. from nadir measurements over clouded scenes ("cloud slicing", Ziemke et al., 2001), or from additional measurements in limb or occultation geometry like SAGE (Fishman and Balok, 1999).

In this study, we focus on stratospheric estimation schemes (SES) for NO_2. The choice of the SES has significant impact on the retrieved tropospheric CDs of NO_2 and leads to systematic differences between different retrievals. Generally, there are

AMTD
2, 2983–3025, 2009

three different approaches for the estimation of stratospheric CDs, using (1) atmospheric chemistry models, (2) a subset of the satellite measurement which represents the stratosphere, and (3) additional (more or less) direct measurements of the stratospheric CD.

(1) Atmospheric chemistry models directly provide information on stratospheric CDs which can be used for the retrieval of tropospheric CDs. Richter et al. (2005) take stratospheric CDs of NO_2 from the SLIMCAT model for their stratospheric estimation. Boersma et al. (2007) use a data assimilation approach with the TM4 model.

While stratospheric NO_x chemistry is in general understood quite well, the utilization of chemistry models for the stratospheric estimation nevertheless has its drawbacks. First, models and measurements generally show no perfect agreement, but typically systematic biases which depend on time, latitude, and/or observation geometry. Hence, model CDs have – somehow arbitrarily – to be "tuned" to match the observations (see Richter et al., 2005). Second, in the case of data assimilation, a-priori knowledge on the global tropospheric NO_2 distribution is needed; in case of a (faulty) stratospheric classification of a signal of tropospheric origin, it would be assimilated in the stratosphere. Third, the resulting tropospheric CDs are no independent measurements any more.

(2) Several approaches of stratospheric correction schemes use the satellite measurements themselves and define subsets, which can be assumed to represent the stratospheric CD, and inter/extrapolate these subsets to global fields afterwards.

A quite simple stratospheric correction scheme for NO_2 is the reference sector method (RSM) (e.g. Richter and Burrows, 2002; Martin et al., 2002; Beirle et al., 2003): The stratospheric CD at a given latitude is estimated from measurements over the remote Pacific (at the respective latitude), which can be considered to be unpolluted. Note that this approach is only applicable for satellites operated in sun-synchonous orbit, so that the *local* time of measurements in- and outside the reference sector is the same. The RSM generally results in tropospheric *excess* CDs w.r.t. the reference sector. Within the RSM approach, longitudinal variations of stratospheric NO_2 are ne-

glected, which generally works well for low and mid-latitudes, but may fail especially at higher latitudes, in particular close to the polar vortices (e.g. Richter and Burrows, 2002; Martin et al., 2002; Boersma et al., 2004; Sierk et al., 2006).

Some refinements of the simple RSM have been discussed, which also allow for longitudinal variations of stratospheric CDs, but still estimate them from the measurements alone. Leue et al. (2001) and Wenig et al. (2004) define unpolluted reference regions around the globe (instead of just one stripe in the Pacific) and interpolate the stratospheric 2D field. Bucsela et al. (2006) perform a Wave-2 fitting along zonal bands. While these refined RSM methods account for longitudinal variations, they have to define (arbitrarily) "unpolluted" regions which must neither be too small (which could lead to interpolation errors and possibly to overshoots of the interpolated stratosphere over the large "polluted" area) nor too large (which could lead to the false classification of a smooth continental tropospheric background in the "unpolluted" region, e.g. from soil emissions, as stratospheric NO_2). These difficulties are amplified in the case of SCIAMACHY due to its poor spatial coverage (compared to GOME/GOME-2 or OMI).

(3) SCIAMACHY is the first satellite instrument which combines limb and nadir measurements. The viewing geometry is alternating between nadir and limb states in such a way, that the atmosphere is first scanned in limb (allowing the retrieval of stratospheric profiles), and afterwards in nadir geometry (giving total CDs for approximately the same air mass) (see Bovensmann et al., 1999). This "Limb-Nadir-Matching" was intended to provide direct measurements of stratospheric CDs corresponding to the successive nadir CD measurements.

For NO_2 and O_3, the potential of SCIAMACHY limb measurements for stratospheric correction has already been demonstrated exemplarily (Sioris et al., 2004; PROMOTE, 2004; Sierk et al., 2006; Heckel et al., 2007). However, to the authors' knowledge, no standard data product of tropospheric NO_2 is retrieved so far involving limb data for stratospheric correction.

Here we discuss the potential of limb measurements for stratospheric correction of total NO_2 CDs. We compare the simple RSM to a direct, absolute limb correction

AMTD
2, 2983–3025, 2009

(ALC), which improves spatial patterns of tropospheric CDs, in particular over and around the polar vortex, but introduces artefacts elsewhere. We present in addition a *relative* limb correction scheme (RLC), where the RSM is applied to the limb data analogue to the nadir data, and the longitudinal variations of limb data is used to correct the tropospheric CDs from simple RSM. This relative correction scheme is simple and robust with respect to possible systematic errors in nadir and/or limb retrievals and their potential dependency on location and time. It is, in essence, free of model input, but based on the satellite measurements.

The RLC scheme is a significant improvement over the simple RSM, yielding more plausible tropospheric NO_2 CDs. In particular over the northern Atlantic, where the RSM in winter results in strong negative tropospheric CDs, the RLC yields realistic tropospheric CDs close to zero. RLC modifications for lower latitudes are less pronounced (compare e.g. Richter and Burrows, 2002; Martin et al., 2002; Boersma et al., 2004), but still significant, over large parts of the continents, even over regions of strong NO_x emissions, like Europe or the US Eastcoast. Thus, the choice of the SES has significant impact of quantitative studies (like emission estimates) based on NO_2 CDs from satellite measurements.

2 Data and methods

In this section we shortly describe the characteristics of the SCIAMACHY instrument (Sect. 2.1) and our retrieval schemes for NO_2 nadir CDs (Sect. 2.2) as well as limb profiles (Sect. 2.3).

We discuss different stratospheric estimation schemes in Sect. 2.4: first (Sect. 2.4.1) the simple reference sector method (RSM), second (Sect. 2.4.2) an absolute limb correction (ALC) scheme, and third (Sect. 2.4.3) a relative limb correction (RLC) scheme. From these three stratospheric estimation schemes, we derive three tropospheric products accordingly (Sect. 2.5), which are compared and discussed in Sects. 3 (results) and 4 (discussion).

AMTD
2, 2983–3025, 2009

In Sect. 2.6 we discuss to which extent information on statistical as well as systematical errors of tropospheric CDs can be gained from the limb/nadir measurements themselves.

The different SES are illustrated for 28 January 2006 exemplarily. Additional examples for other times of the year, as well as a more in-depth discussion of error quantities, are presented in a supplementary document (how to refer?), referred simply as "Supplement" hereafter (see http://www.atmos-meas-tech-discuss.net/2/2983/2009/amtd-2-2983-2009-supplement.pdf).

Table 1 gives an overview on the symbols and abbreviations used in this study.

2.1 SCIAMACHY

The Scanning Imaging Absorption Spectrometer for Atmospheric CHartographY, SCIAMACHY (Bovensmann et al., 1999), was launched onboard the ESA satellite ENVISAT in March 2002. ENVISAT orbits the Earth in a sun-synchronous orbit with an inclination from the equatorial plane of 98.5°. It performs one orbit in approx. 100 min, with a local equator crossing time of about 10:00 a.m. in descending node.

SCIAMACHY measures Earthshine spectra from the UV to the NIR with a spectral resolution of 0.22–1.48 nm. It is operated in different viewing geometries, like nadir, limb, or solar/lunar occultation. In nadir geometry (i.e. directed vertically, perpendicular to the Earth's surface), the instrument performs an across-track scan of about ±32°, equivalent to a swath-width of 960 km. The footprint of a single nadir observation is typically $30 \times 60\,km^2$. Global cover of nadir measurements is achieved after 6 days. In limb geometry (i.e. directed horizontally, tangential to the Earth's surface), the instrument performs scans in flight direction with elevation steps of approx. 3.3 km at the tangent point. The cross-track swath is 960 km, as for the nadir measurements, and consists of up to 4 pixels. The field of view at the tangent point is about 2.5 km (vertically) ×110 km (horizontally). The limb scanning allows the retrieval of stratospheric profiles of NO_2 (see Sect. 2.3).

AMTD
2, 2983–3025, 2009

In standard operation, the measurement state is alternating between limb and nadir in such a way that the limb measurements probe (almost) the same stratospheric air mass as the subsequent nadir measurements. Note that the term "state" in the following is used to denote the SCIAMACHY measurement mode as well as to summarize the entity of measurements performed within one nadir/limb state.

2.2 Retrieval of total slant column densities of NO_2: nadir

Slant column densities (SCDs) S of NO_2 are derived from SCIAMACHY nadir spectra using Differential Optical Absorption Spectroscopy DOAS (Platt and Stutz, 2008). Cross-sections of O_3, NO_2, O_4, H_2O and Glyoxal are fitted in the spectral range 430.8–459.5 nm. In addition, Ring spectra, accounting for inelastic scattering in the atmosphere (rotational Raman) as well as in liquid water (vibrational Raman), an absorption cross-section of liquid water, and a polynomial of degree 5 are included in the fit procedure. A daily solar measurement is used as Fraunhofer reference spectrum.

This NO_2 DOAS retrieval setup is different from previous versions (e.g. Beirle, 2004) in so far that liquid water absorption and vibrational Raman scattering on liquid water molecules is now accounted for, which have been shown to affect spectra in the UV/vis (Vasilkov et al., 2002; Vountas et al., 2007). This modification improves the spectral fits over oligotrophic oceanic regions (Polovina et al., 2008), where NO_2 SCDs of the previous fit version show a systematic negative bias. The remaining (but significantly smaller) systematic spatial patterns over oligotrophic oceanic regions are subject to further investigations. These effects are related to this study in so far that large parts of chosen reference region in the Pacific cover oligotrophic regions. With the current settings, the remaining biases over oceans are rather small (see discussion); information on possible systematic effects is contained in the standard deviation of NO_2 CDs in the RS (see Sect. 2.6).

For this study, we only consider measurements of the descending part of the orbit with solar zenith angles (SZA) $\alpha < 80^\circ$, since for higher SZA, the sensitivity for the troposphere becomes rather small. No cloud filter is applied, since in this study, our aim

is an improved stratospheric estimation scheme, and the impact of clouds on stratospheric CDs is negligible.

2.3 Retrieval of stratospheric NO_2 profiles: limb

An algorithm for the retrieval of NO_2, BrO and OClO vertical profiles from SCIAMACHY limb measurements was developed in our group (Puķīte et al., 2006; Kühl et al., 2008). The retrieval is performed in two steps: In the first step, SCDs are derived from the SCIAMACHY limb spectra at different tangent heights by DOAS. For NO_2 the fit-window ranges from 420 to 450 nm. As reference spectrum we apply a measurement at a tangent height where the absorption of the considered trace gas is small, i.e. for NO_2 at ~42 km.

Second, the trace gas SCDs are converted into a vertical concentration profile by an inversion scheme based on a least squares approach (see e.g. Menke, 1999). To increase the signal-to-noise ratio, only one averaged SCD per tangent height is applied for the inversion (i.e. the SCD results of the four measured spectra per tangent height are co-added).

For the inversion, box AMFs are calculated with the 3-D fully spherical Monte Carlo RTM "McArtim" (Deutschmann, 2009), using temperature, pressure and ozone data from a model simulation provided by Brühl and Crutzen (1993). It should be noted that in some individual cases the actual temperature, pressure and ozone profile might differ considerably from the assumed model profiles. No aerosols and clouds are assumed for the calculation of the box AMFs. The aerosol extinction is much lower compared to extinction by Rayleigh scattering in the stratosphere. Also, due to the slantness of limb observations, SCDs derived from measured spectra are practically insensitive to the atmosphere below the tangent height.

From sensitivity studies it was found that the related errors in the profile retrieval are of the order of some percents in the upper and middle stratosphere (i.e. where the peak of NO_2 occurs) but can be up to 30% for altitudes around 15 km.

AMTD
2, 2983–3025, 2009

In comparison studies a good agreement of the retrieved BrO and NO_2 profiles with correlated balloon validation measurements was found (Dorf et al., 2006; Butz et al., 2006; Kühl et al., 2008; Puķīte et al., 2009a).

For the algorithm details please refer to Puķīte et al. (2006) and Kühl et al. (2008).

2.4 Stratospheric estimation schemes (SES)

The DOAS algorithm as described in Sect. 2.1 yields total SCDs S of NO_2. The slant column density S is the concentration integrated along the effective light path. It is usually converted into a vertical column density (VCD) V, i.e. the vertically integrated concentration, via the air-mass factor (AMF) A:

$$V = S/A. \quad (1)$$

The air-mass factor has to be calculated by radiative transfer models and depends on observation geometry (SZA and LZA), ground albedo, aerosols, clouds, and the trace gas profile. The dominant dependencies are fundamentally different for stratospheric and tropospheric trace gases. For the considered nadir observations with SZA below 80°, stratospheric AMFs mainly depend on observation geometry and are thus well determined. Tropospheric AMFs, however, critically depend on ground albedo, clouds, aerosols, and the tropospheric trace gas profile, i.e. several parameters which have to be considered as external input.

In this study, we focus on quantifying the effect of different stratospheric estimation schemes (SES) on tropospheric column densities. For this purpose, we define V^* by applying stratospheric AMFs to the total SCDs:

$$V^* := S/A_{\text{Strat}}, \quad (2)$$

where stratospheric AMFs A_{Strat} are calculated as function of SZA α and LZA β using the RTM McArtim (Deutschmann, 2009).

The asterisk should indicate that these VCDs cannot be interpreted quantitatively as total VCDs, since the tropospheric fraction of the SCD was converted (inappropriately)

with a stratospheric AMF. This has to be kept in mind for the interpretation of tropospheric residues and will be corrected below (2.5) by multiplication with A_{Strat}, yielding tropospheric SCDs.

For the retrieval of tropospheric CDs (see next section), first the stratospheric CD W has to be estimated and removed from the total CDs. In the following we describe three different stratospheric estimation schemes: 1. a classical, simple Reference Sector Method (RSM), and 2./3. two SES involving limb data, i.e. an absolute limb correction (ALC), and a relative limb correction (RLC). The different SES are discussed exemplarily for 28 January 2006 below. Additional examples for other days are shown in the supplement.

2.4.1 Reference Sector Method (RSM)

The basic idea of the simple RSM is that the stratospheric VCD at any place can be estimated by the total VCD over a remote region (typically the Pacific) of the same latitude. I.e., the RSM assumes that (a) a sufficiently clean reference sector (RS) with negligible tropospheric pollution can be defined, and (b) the global stratospheric VCD field does only depend on latitude Λ, but not on longitude Φ.

We follow this simple approach by defining a RS in the Pacific as indicated in Fig. 1, showing V^* for 28 January 2006. For every day d, we calculate a look-up table (LUT) $V^*_{\mathrm{RS}}(d,\Lambda)$ by averaging the daily measurements V^* over the RS in latitudinal bins of 1° resolution.

A smoothed LUT $\widehat{V}^*_{\mathrm{RS}}(d,\Lambda)$ is derived by convoluting $V^*_{\mathrm{RS}}(d,\Lambda)$ with Gaussian functions both in temporal ($\sigma = 5$ days) and in latitudinal ($\sigma = 5°$) dimension. Both the non-smoothed ($V^*_{\mathrm{RS}}(d,\Lambda)$) and the smoothed LUT $\widehat{V}^*_{\mathrm{RS}}(d,\Lambda)$ are shown in Fig. S1 of the supplement (see http://www.atmos-meas-tech-discuss.net/2/2983/2009/amtd-2-2983-2009-supplement.pdf). For the sample day 28 January 2006, V^*_{RS} and $\widehat{V}^*_{\mathrm{RS}}$ are also displayed as function of latitude in Fig. 3 in direct comparison to the Limb VCDs in the RS (see next section).

AMTD
2, 2983–3025, 2009

For the RSM, we define the stratospheric VCD W_{RSM} as function of day d and latitude Λ as:

$$W_{\mathrm{RSM}}(d,\Lambda) := \widehat{V}^{*}_{\mathrm{RS}}(d,\Lambda). \quad (3)$$

2.4.2 Absolute Limb Correction (ALC)

Stratospheric Limb VCDs (LVCDs) L are calculated from the derived limb concentration profiles (see Sect. 2.2) by simply integrating the profiles from 15 km to 42 km. Varying the lower integration limit between 12 km and 18 km affects the resulting LVCDs by less then 5%. We therefore neglect the latitudinal variation of tropopause height in this study. Errors of L are derived from integrating the uncertainties of the concentration in each layer as derived by the limb inversion. A LVCD error threshold of 0.25×10^{15} molec/cm^2 is defined to eliminate outliers, which mainly occur due to the South Atlantic Anomaly.

Due to the co-adding of the four horizontal limb scans, one limb VCD L is available per limb state. Due to the alternating limb/nadir measurements, a single L could be used as (constant) stratospheric estimation for all measurements within the according nadir state, as in Sierk et al. (2006). However, in doing so, a single biased L would affect a complete nadir state. In addition, the assumption of a constant stratosphere within one nadir state leads to artificial step functions in the latitudinal dependency of the resulting TSCDs. We thus use the individual Limb VCDs L to calculate a smooth LUT $\widehat{L}(d,\Lambda,\Phi)$ by folding with Gaussian functions $G(\sigma_{\mathrm{lon}},\sigma_{\mathrm{lat}})$ with $\sigma_{\mathrm{lon}} = 20^{\circ} \times \cos(\Lambda)$ and $\sigma_{\mathrm{lat}} = 10^{\circ} \approx 1000$ km. These settings for σ_{lon} force smooth spatial patterns for low latitudes ($\sigma_{\mathrm{lon}} = 20^{\circ} \approx 2000$ km at the equator) and allow strong longitudinal gradients only at higher latitudes ($\sigma_{\mathrm{lon}} = 10^{\circ} \approx 500$ km at 60° latitude), having in mind that especially at the polar vortex, strong longitudinal gradients of stratospheric NO_2 CDs do occur.

To improve statistics and to avoid large spatial gaps, generally limb measurements of the previous and following day are included with half weight in the folding procedure.


In addition, all limb CDs are weighted by the inverse square of their error.

Figure 2 shows a global map of limb VCDs on 28 Jan 2006. The location of the limb tangent points of individual LVCDs are marked by colour-coded disks, while the background map displays the smoothed LUT $\widehat{L}(d,\Lambda,\Phi)$. Keep in mind that for the retrieval of the profile at the tangent point, all limb scans within the limb state are used for the inversion, which cover an area of about thousand km extent both in latitudinal as in longitudinal direction. The latitudinal dependency of L selected over the RS on 28 January 2006 is added in Fig. 3 for an absolute comparison to the RS VCDs V^*_{RS} from nadir observations.

For the absolute limb correction scheme, we define the stratospheric VCD as

$$W_{\mathrm{ALC}}(d,\Lambda,\Phi) := \widehat{L}(d,\Lambda,\Phi). \quad (4)$$

2.4.3 Relative Limb Correction (RLC)

As illustrated in Fig. 3, L_{RS} and V^*_{RS}, i.e. W_{RSM} and W_{ALC} over the reference sector, show generally similar latitudinal dependencies, but still reveal significant differences, depending on latitude. As will be shown below, this leads to non-realistic zonal stripes in the corresponding tropospheric CD product. In particular, L is often higher than V^*, leading to negative tropospheric CDs.

Thus, we also perform a *relative* limb correction, which by definition eliminates the deviations of limb and nadir VCDs in the RS. The basic idea is to apply the same RS correction that was applied for the nadir VCDs also to the limb VCDs: from the limb VCDs L over the RS we derive a LUT $\widehat{L}_{\mathrm{RS}}(d,\Lambda)$, which again is smoothed over time and latitude.

The difference of L and $\widehat{L}_{\mathrm{RS}}$ at the same day and latitude holds information on longitudinal variations for a given latitude:

$$\Delta L(d,\Lambda,\Phi) = L(d,\Lambda,\Phi) - \widehat{L}_{\mathrm{RS}}(d,\Lambda). \quad (5)$$

AMTD
2, 2983–3025, 2009

We thus denote ΔL as Limb Longitudinal Variation (LLV). Figure 4 displays the individual ΔL at the limb tangent points as disks, while the background map shows $\widehat{\Delta L}$ which was smoothed with the same settings as $\widehat{L}$ (see Sect. 2.4.2). Again, measurements of the previous and following day are included with half weight.

Now we use $\widehat{\Delta L}$ to define the relative limb correction stratospheric VCD as the classical RSM VCD modified by longitudinal variations as observed by the limb measurements:

$$W_{\mathrm{RLC}}(d,\Lambda,\Phi) := W_{\mathrm{RSM}}(d,\Lambda) + \widehat{\Delta L}(d,\Lambda,\Phi). \quad (6)$$

Figure 5 compares global maps of stratospheric VCDs W for the three SES for 28 January, 2006.

2.5 Tropospheric SCDs of NO_2

With these estimates W for stratospheric VCDs of NO_2, we can define the tropospheric residue as

$$\Delta V^* := V^* - W. \quad (7)$$

ΔV^* represents the *tropospheric* VCD derived with a *stratospheric* AMF. Due to the strong dependency of A_{Strat} on observation geometry, ΔV^* strongly depends on SZA and LZA, which is not realistic for tropospheric VCDs. To correct this inconsistency, we re-transfer ΔV^* back to a tropospheric *slant* column density T:

$$T := \Delta V^* \times A_{\mathrm{Strat}}. \quad (8)$$

From T, a tropospheric VCD could be derived directly by division with the appropriate tropospheric AMF. Within this study, however, we do not apply tropospheric AMFs, since we want to focus solely on the effect of different SES, without involving (and discussing the impact of) external datasets (for ground albedo, clouds/aerosols and profiles). For orientation, however, note that tropospheric AMFs for cloud free scenes

AMTD
2, 2983–3025, 2009

are of the order of 1 (Richter and Burrows, 2002), and generally <1 for clouded scenes, except for cases with substantial NO_2 within/above the cloud.

So, all total CDs (V^*) and all stratospheric CDs (W) presented in this study are vertical column densities, while the tropospheric CDs T discussed below are slant column densities. This differentiation is potentially confusing, but necessary, since stratospheric CDs need to be processed in terms of VCDs (e.g. for the averaging of RS column densities of the same latitude for different SZA/LZA), but the relevant tropospheric CDs, prior to the application of tropospheric AMFs, are slant column densities. Thus, we discuss the effect of the different SES on tropospheric CDs in terms of SCDs in Sects. 3 and 4. The stratospheric AMF, i.e. the ratio of T and ΔV^*, is slightly above 2 for low SZA (tropics) up to 7 for high SZA (80°).

The resulting TSCDs for the three different SES are displayed in Fig. 6. Note that both T_{RSM} and T_{RLC} are by definition tropospheric excess CDs (relative to the reference sector), while T_{ALC} in principle should result in absolute total tropospheric CDs.

2.6 Intrinsical error information

In this section we briefly discuss the potential of detecting and estimating systematic as well as statistical errors from the measurements themselves. A more in-detail discussion of this issue, and the actual definition of the terms we use for quantitative error information, are given in the supplement (Sect. S3: http://www.atmos-meas-tech-discuss.net/2/2983/2009/amtd-2-2983-2009-supplement.pdf).

Estimates of the accuracy of TSCDs can be derived from the TSCDs themselves in so far, that systematic negative TSCDs (on a level beyond possible statistical fluctuations around zero) are definitively unphysical. Also strange spatial patterns of TSCDs far from known NO_x sources may indicate shortcomings of the SES. Finally, if a SES is insufficient, fluctuations of the remaining stratospheric features lead to enhanced standard deviations (over time) of the resulting TSCDs. Thus, the success of an advanced SES has to be demonstrated by an improvement of accuracies, i.e. the removal/reduction of a) systematic negative TSCDs, b) strange spatial features which

AMTD
2, 2983–3025, 2009

are obviously not of tropospheric origin, and c) TSCD standard deviations (over time).

Additional information on both statistical and systematic errors can be derived from the standard deviation (over longitude) of W in the reference sector. This quantity comprises statistical errors (e.g. from the DOAS fit error and natural fluctuations of stratospheric VCDs), but enhanced values clearly indicate additional systematic errors, e.g. due to fit artefacts over oligotrophic oceanic regions.

From the comparison of individual LLV ΔL to the smoothed LUT $\widehat{\Delta L}$, information on the performance of the smoothing/interpolation procedure can be derived, which is in particular limited in cases of strong temporal and spatial gradients.

In Sect. S3 of the supplement (see http://www.atmos-meas-tech-discuss.net/2/2983/2009/amtd-2-2983-2009-supplement.pdf), we define and display the error quantities δW_{RSM} and δW_{RLC}, which are automatically calculated during the TSCD retrieval, and are provided as function of day and latitude. Thus, though shortcomings of the RLC SES remain for some regions/times, these can be recognized by enhanced values of δW_{RSM} or δW_{RLC}.

3 Results

In this section, we present TSCDs for the different SES, and analyze their specific characteristics and differences. Again, we focus on wintertime, where the shortcomings of the RSM are emerging particularly. Results for other times of the year are presented in the Supplement and also shortly discussed below.

Figure 6 shows the resulting TSCDs T_{RSM}, T_{ALC}, and T_{RLC} for 28 January 2006 exemplarily. Note that the colorscale has been chosen to accentuate small systematic deviations – in particular negative ones – from 0 over "clean" regions. Polluted regions like Europe, the US eastcoast, or China, are by far in saturation.

As can be seen in Fig. 4, the simple assumption of a zonally constant stratospheric CD is not valid. As a consequence, the RSM leads to – unphysically – negative TSCDs T_{RSM} (Fig. 6a) over the Northern Atlantic down to -2×10^{15} molec/cm^2, which is far

below the statistical uncertainty. In contrast, T_{RSM} over wide areas in remote Northern Asia is quite high. Similar shortcomings of the RSM in wintertime have been discussed in e.g. Richter and Burrows, 2002, or Sierk et al., 2006.

The ALC (Fig. 6b) significantly improves the patterns over the North Atlantic, and the strong negative bias is successfully corrected. However, T_{ALC} shows strong zonal features, both positive and negative: oceanic CDs around the equator are negative now (in contrast to T_{RSM}) about -1×10^{15} molec/cm^2, and T_{ALC} is unrealistically high (2×10^{15} molec/cm^2) south of 60° S, i.e. far from any known source of NO_x. This is a direct consequence of the different latitudinal dependencies of V^*_{RS} and L_{RS} (Fig. 3), which reveals systematic deviations that lead to negative (20° S to 20° N) as well as positive (south of 60° S) background TSCDs T_{ALC}. Keep in mind that Fig. 3 displays VCDs; the differences in TSCD (Fig. 6b) are higher by AMF_{Strat}, which is about 2 in the tropics up to 7 at high latitudes.

The RLC results in the most plausible NO_2 TSCDs (Fig. 6c). T_{RLC} shows a clear improvement of spatial patterns compared to T_{RSM}: the negative T_{RSM} over the North Atlantic are corrected in T_{RLC}, and also other regions with negative T_{RSM} (e.g. South-East from Japan) are more plausible in T_{RLC}. At the same time, the artificial zonal features introduced by the ALC are eliminated by the RLC: in contrast to T_{ALC}, T_{RLC} is – per definition – still 0 on average over the RS.

The longitudinal variations in T_{RSM} at about 60° S are reduced in T_{RLC}, but could not be removed completely by the RLC. Generally, patterns at Northern mid– and high latitudes are corrected successfully by the RLC, but are only lessened in the Southern Hemisphere (see additional examples in the supplements and discussion).

After illustrating the different TSCDs for a specific day, we compare monthly climatologies (mean 2003–2008) of TSCDs for January (Fig. 7) and additional months in the supplements (Figs. S11–S16). Obviously, the longitudinal variations of stratospheric NO_2, as observed for 28 January 2006, do not cancel out by temporal averaging, but instead systematic spatial patterns stand out.

Mean January T_{RSM} (Fig. 7) is negative up to -2×10^{15} molec/cm^2 over large parts of

AMTD
2, 2983–3025, 2009

Canada and the North Atlantic, and quite high ($> 1 \times 10^{15}$ molec/cm^2) throughout North-Eastern Russia. As for the individual day, the ALC reduces/removes these longitudinal variations, but introduces zonal stripes of negative TSCDs around the equator, and high positive TSCDs south of 60° S (Fig. 7b). Again, T_{RLC} improves the longitudinal variations while retaining the RS levels to 0 on average (Fig. 7c).

The differences of the mean TSCDs are shown in Fig. 8, directly illustrating the effects of the different stratospheric estimation schemes. Compared to T_{RSM}, both ALC (Fig. 8a) and RLC (Fig. 8b) have removed a similar dipolar pattern with a maximum amplitude of 2.5×10^{15} molec/cm^2 at northern latitudes. However, the ALC introduces zonal stripes in the climatology up to 1.2×10^{15} molec/cm^2 over the RS at the equator (Fig. 8a and c). In contrast, the difference $T_{RSM} - T_{RLC}$ is negligible for latitudes between 30° N and 60° S.

Note that T_{ALC} and T_{RLC} show different longitudinal dependencies (see the local pattern over South America in Fig. 8c), which would on first view not be expected, since the longitudinal dependencies of both, W_{ALC} and W_{RLC}, are derived from the limb measurements only. The reason for the observed differences in longitudinal behaviour is the calculation of $\widehat{\Delta V}$, which is derived from smoothing the individual ΔV, instead performing the RS correction to $\widehat{V}$; this is a non-commutative procedure. The difference over South America is outstanding, since most limb observations are skipped there, as a consequence of high errors of L due to the South Atlantic Anomaly.

Besides the effect of the different stratospheric estimation schemes on mean values, we also analyzed the standard deviations s of TSCDs over time for January 2003–2008 (Fig. 9). As expected, standard deviations are generally high over polluted regions, where mean TSCDs are enhanced, due to variability of tropospheric CDs. Beyond that, however, $s(T_{RSM})$ is high ($> 3 \times 10^{15}$ molec/cm^2) over the Northern Atlantic, in constrat to $s(T_{ALC})$ and $s(T_{RLC})$. Figure 10, showing the differences of standard deviations, reveals that both T_{ALC} and T_{RLC} lead to lower standard deviations over large areas at high latitudes. The consideration of longitudinal variations from limb measurements thus clearly reduces the standard deviations by about 1 up to 3×10^{15} molec/cm^2 com-

AMTD
2, 2983–3025, 2009

pared to the simple RSM. Note that standard deviations of T_{ALC} and T_{RLC} are almost identical (Fig. 10c), despite their differences in mean values. This indicates that $s(T_{ALC})$ is driven by tropospheric variability and stratospheric dynamics, but *not* by the zonal stripes introduced by the ALC, which are thus rather constant in magnitude and location for a fixed month.

Figures S4–S16 of the Supplement (see http://www.atmos-meas-tech-discuss.net/2/2983/2009/amtd-2-2983-2009-supplement.pdf) illustrate that the RLC improves the spatial patterns both on individual days as well as in monthly climatologies also for other times of the year. Typical values for daily LLVs (in terms of VCD) are below $\pm 0.3 \times 10^{15}$ molec/cm^2 for low latitudes, but can reach ± 0.6 up to 1×10^{15} molec/cm^2 for higher latitudes in some months (Figs. S4, S6, S8). Figure S10 illustrates that the principal shortcoming of the ALC, caused by different latitudinal dependencies of V^* and L, and L being generally higher than V^*, is present throughout the year.

For the monthly climatologies, the RLC modifies the resulting TSCDs by less than 0.5×10^{15} molec/cm^2 for low and midlatitudes, and up to 1×10^{15} molec/cm^2 at high northern latitudes (about 60°) in April and October. In October, the difference $T_{RSM} - T_{RLC}$ is up to 3×10^{15} molec/cm^2 at 60° S, and still unrealistic spatial patterns (negative T_{RLC}) are present (Figs. S15–16). Thus, especially for the Southern Hemisphere, the RLC sometimes rather reduced than completely removes the artefacts of the RSM. Nevertheless, standard deviations of T_{RSM} are always significantly reduced by the RLC (Figs. S12, S14, S16).

After discussing global maps of TSCDs for the different SES for different days/months, we also investigate the temporal pattern as well as frequency distributions of TSCDs for four selected locations: two in the Northern Hemisphere (50° N) and two in the Southern Hemisphere (50° S) at 20° W and 110° E, respectively. All locations are remote, far from known sources of NO_x, and are considered to be "clean". They are marked by crosses in Figs. 6–10.

Figure 11 shows the annual cycles of the different TSCDs. Figure 12 displays the respective frequency distributions and list means and standard deviations for these

locations.

The first location (20° W, 50° N) is located in the Northern Atlantic. RSM TSCDs T_{RSM} (blue) are often negative and generally show a high variability in winter. This variability is reduced both in T_{ALC} (green) and T_{RLC} (orange). However, T_{ALC} shows systematically higher CDs in summer. While the mean of T_{RSM} is negative, T_{RLC} is almost zero. The standard deviations both of T_{ALC} and T_{RLC} are reduced compared to T_{RSM}.

The second location, placed in Russia (110° E, 50° N) far from large cities, wintertime T_{RSM} is quite high (up to 5×10^{15}). On average, T_{RSM} is 0.67×10^{15} molec/cm^2. ALC reduces these high wintertime TSCDs, but introduces too high TSCDs in summertime. T_{RLC} is close to zero on average and has a reduced standard deviation.

The Southern hemispheric locations, (20° W and 110° E, 50° S) are over Ocean, far from known NO_x sources. The annual cycle and frequency distributions of both southern locations are similar: T_{RSM} shows high variability and high CDs in SH winter (NH summer). T_{ALC}, is overcorrecting the SH wintertime TSCDs, resulting in negative TSCDs down to -5×10^{15} molec/cm^2. Again, T_{RLC} is close to zero on average and has a reduced standard deviation.

For all considered clean locations, mean T_{RLC} is non-negative, close to zero, and its standard deviation is lowest, indicating RLC being the most realistic SES.

4 Discussion

Estimating the stratospheric column density over a remote reference sector is an easy, robust method for the retrieval of tropospheric CDs, and has been used successfully in several studies on tropospheric NO_2. In particular, it implies a first-order correction of any systematic offset in total CDs. The simple assumption of zonal constancy, however, clearly fails at higher latitudes, in particular close to the polar vortex. We present two advanced stratospheric estimation schemes (ALC and RLC) involving additional limb measurements and apply them to 6 years of SCIAMACHY measurements.

AMTD
2, 2983–3025, 2009

Stratospheric correction by ALC generally improves spatial patterns of TSCDs compared to the RSM with respect to longitudinal variations. However, in the resulting TSCDs T_{ALC}, systematic zonal stripes (about $\pm 1 \times 10^{15}$ molec/cm^2 in monthly climatologies) show up, as a consequence of different latitudinal dependencies of V^*_{RS} and L_{RS}. Generally, L is *higher* than V^* for low/mid latitudes most time of the year, resulting in negative T_{ALC}. Low or even negative tropospheric CDs, resulting from subtraction of stratospheric limb VCDs, can also be seen in Sioris et al. (2004) (Fig. 6 therein) and in PROMOTE (2004).

The following aspects might lead to systematic biases in either nadir or limb data, thus potentially causing different latitudinal dependencies:

- Total nadir SCDs might be biased due to artificial spectral structures in the direct solar reference measurement, caused by the optical system (diffusor plate). However, the observed zonal stripes can not be eliminated by simply adding a constant offset to total SCDs.

- In our analysis, we define the limb VCD L as the integrated limb concentration from 15 km to 42 km. We thereby neglect latitudinal variations of the tropopause height (TH), and thus generally tend to overestimate L over the tropics, and underestimate it at high latitude. However, these effects are far too small ($< 5\%$ for TH between 12 and 18 km) to explain the different latitudinal dependencies of V^* and L seen in Fig. 2 and Fig. S10.

- Though limb and nadir measurements are performed from the same platform, there is a time shift of about 7 min between the limb- and the nadir sounding of the stratosphere. Shortly after sunrise, this may be long enough for significant differences of NO_2 due to changes in photochemistry.

- The effects of clouds and aerosols are ignored in the retrieval of limb profiles. The neglection of high clouds (e.g. over the ITCZ) results in an underestimation of box AMFs in and above the clouds. However, the total limb column would only be

affected significantly, if there would be high NO_2 concentrations in/directly above the cloud.

– Clouds potentially affect the nadir total SCDs by their impact on the Earth shine spectra, e.g. via their impact on polarization, the probability of inelastic scattering (Ring effect), or the shielding of light reflected at the ground, carrying spectral albedo information. The latter could be important especially over the problematic oligotrophic oceanic regions. However, we find no correlation of TSCDs and cloud fraction ($R = -0.01$ for 28 January, 2006, over the RS).

– In addition, clouds lead to increased stratospheric AMFs, which is only a small effect (< 2%) and thus not considered in this study.

– The limb inversion scheme is based on one dimensional RTM, assuming horizontal homogeneity. In cases of horizontal gradients, this leads to errors in the resulting profiles, since the effective light paths for low tangent heights do not reach as close to the tangent point as for high tangent heights. This leads to errors up to 20% for NO_2 at the polar vortex (Puķīte et al., 2008). A SCIAMACHY operation change request (OCR #38) was approved and performed: In December 2008, several successive orbits have been operated in exclusive limb geometry. This allows us to investigate and quantify 3-D effects also for midlatitudes and tropics as well as for the Southern Hemisphere (Puķīte et al., 2009b).

These and possibly other factors with latitudinal dependency (which may also be the consequence of a SZA dependency) have systematic impact on V^* and/or L. The in-detail comparison of the latitudinal dependencies of V^* and L thus can help to indicate and quantify shortcomings of the nadir and/or limb retrievals in future studies. However, as shown in this study, the direct ALC is not appropriate for an automatized retrieval of NO_2 TSCDs up to now.

A third method, the RLC, was quite successful in removing longitudinal variations without the drawbacks of the ALC. By applying the RSM to nadir and limb data likewise,

an absolute calibration of vertical column densities (limb and nadir) is not required, and systematic biases are first-order corrected. Also possible jumps in the time series (due to e.g. calibration setting changes) and degradation effects are automatically corrected for. The RLC thus keeps the heritage of the RSM, i.e. being a simple, robust, and model independent correction scheme, but clearly improves spatial patterns of the resulting TSCDs, where longitudinal variation let the RSM fail. T_{RLC} shows generally means close to 0 and lowest std over clean regions. The RLC introduces changes in TSCD (compared to RSM) up to 3×10^{15} molec/cm^2 for some months (January, Fig. 8b; October, Fig. S16a), while in Northern hemispheric summer, changes are generally low ($< 0.5 \times 10^{15}$ molec/cm^2 for July, Fig. S14a).

However, while the RLC is a significant improvement over the simple RSM, it is not capable of eliminating stratospheric features completely. In particular for the Southern Hemisphere, spatial patterns, that are obviously not of tropospheric origin, remain in maps of T_{RLC}. Possible reasons for these specific SH shortcomings are:

- Especially in the Southern Hemisphere, very localized stratospheric features occur. For instance, on 24 October, 2005, a small filament of enhanced NO_2 CDs is visible in the map of V^* south of Africa (see Figs. S8 and S9 of the Supplement, http://www.atmos-meas-tech-discuss.net/2/2983/2009/amtd-2-2983-2009-supplement.pdf). Limb VCDs L for this region are also enhanced, i.e. the observed NO_2 is located in the stratosphere. Though the limb measurements are capable of detecting this feature, however, they can not fully resolve the spatial structure of this filament due to their coarse spatial resolution (one profile per state). This inevitably leads to an incomplete correction of T_{RLC} of this structure (see Fig. S9c). However, this shortcoming is reflected by a high value for δW_{RLC} (and thus δT_{RLC}), which regularly occurs in autumn at 60°S (Fig. S3).

- Limb measurements are performed in forward direction, i.e. southwards for the descending orbits. I.e., at high northern latitudes, limb measurements “look” from

high to low SZA, with the sun ahead, and vice versa at high southern latitudes. This is a systematic difference of the observation geometries of both hemispheres which may at least partly explain why the RLC works less successful in the SH.

One remaining possible shortcoming of both RSM and RLC are systematic biases of total nadir SCDs due to spectral interference of water absorption and vibrational Raman scattering. This potentially affects the stratospheric estimation around 30° S, with impact on tropospheric CDs over southern South America, South Africa, and Australia. From the spatial variations of NO_2 in and out of oligotrophic oceanic regions, we estimate this bias to be below 0.5×10^{15} molec/cm^2 (in terms of TSCDs). Further improvements of the spectral fit are purpose of ongoing studies.

TSCDs from RSM and RLC are, by definition, tropospheric *excess* CDs w.r.t. the reference sector, i.e. neglecting the small, but existent levels of tropospheric NO_2 SCDs of the order of $0.3–0.6 \times 10^{15}$ molec/cm^2, depending on latitude (Martin et al., 2002). For quantitative interpretation of T_{RSM} and T_{RLC}, this has to be considered by adding modelled Pacific TSCDs, like in Martin et al. (2002). Alternatively, for comparisons of T_{RLC} ("pure" measurement) to modelled TSCDs, the same RS correction could be applied to the latter (Franke et al., 2009).

The changes in TSCDs between the different SES are significant, and have strong impact of quantitative studies on tropospheric NO_2, like emission estimates. In particular over Siberia, RLC leads to TSCDs that are lower compared to T_{RSM} by about 1 to 2×10^{15} molec/cm^2 in a climatology for January 2003–2008. Over Europe, on the other hand, T_{RLC} is higher by about 1×10^{15} molec/cm^2 than T_{RSM}. Over polluted European sites, mean wintertime TSCDs reach values of about 4×10^{15} molec/cm^2 (Paris) up to $> 10 \times 10^{15}$ molec/cm^2 (Milano) (on a $0.5° \times 0.5°$ grid), i.e. the RLC SES has significant impact on TSCDs even at polluted sites. For hemispheric spring and summer, effects are generally smaller, but still systematic differences of RSM and RLC of the order of $0.2–0.4 \times 10^{15}$ molec/cm^2 occur over large areas.

AMTD
2, 2983–3025, 2009

Though the RSM is an established SES, our study emphasizes the need to account for longitudinal variations of stratospheric NO_2. This affects also studies on relative signals (e.g. the Sunday reduction/weekly cycle), as the RSM bias is additive, not multiplicative. In particular, studies on NO_2 in remote regions at high latitudes with relatively low TSCD levels, e.g. soil emission estimates over deserted regions like Siberia, have to keep in mind urgently the impact of the stratospheric estimation and the related uncertainties.

5 Conclusions

In this study, we analyzed different estimation schemes for stratospheric column densities, involving limb measurements from the SCIAMACHY instrument, for the improvement of tropospheric CD retrievals of NO_2.

Estimating the stratospheric CDs by a simple Reference Sector Method (RSM), which is generally a robust and successful method, leads to systematic errors in stratospheric VCDs. Consequently, TSCDs T_{RSM} are negative over the Atlantic (50° N) down to -4×10^{15} (daily extreme)/-1×10^{15} molec/cm^2 (monthly climatology) in autumn/winter months.

A direct, absolute limb correction (ALC) is capable of correcting longitudinal variations of stratospheric CDs, thus being an improvement compared to the simple Reference Sector Method at high latitudes. However, the latitudinal dependencies of limb and nadir CDs turned out to be systematically different, making an automatized retrieval of tropospheric CDs by the ALC inappropriate.

Instead, we developed a relative limb correction (RLC) scheme which successfully improve the RSM w.r.t. longitudinal features, without introducing artefacts elsewhere, and suggest to use this scheme for the retrieval of NO_2 TSCDs. This correction scheme keeps the heritage of the simple RSM, i.e. it is based on measurements and free of a-priori assumptions on NO_x emissions or modelled stratospheric CDs etc., but significantly improves the shortcomings of the RSM. The spatial patterns of the TSCDs

AMTD
2, 2983–3025, 2009

derived by RLC are much more plausible (i.e. closer to zero for clean regions) than for RSM and ALC, and show lowest standard deviations of TSCDs w.r.t. time.

However, though the RLC generally works successfully, spatial features of stratospheric origin partly remain in tropospheric CDs, especially for high Southern latitudes. But regions south of 50° S are generally irrelevant for studies of tropospheric NO_2.

The definition of error quantities δW and δT provides information on statistical and especially systematic errors, which are calculated automatically in the TSCD retrieval, and provided as function of day and latitude. In particular, enhanced values of δW_{RSM} indicate shortcomings of the DOAS fit over oligotrophic oceans, while enhanced values of δW_{RLC} are observed for scenarios with high spatial gradients of stratospheric NO_2 which are not resolved by the limb measurements.

The available dataset on limb longitudinal variations can be used to check and improve other SES, in particular advanced RS methods working with 2-D interpolation or wave fitting. This is important for current and future satellite instruments without the limb viewing mode.

The RLC was discussed for NO_2 in this study. Generally, it could also be applied to other trace gases like O_3. For such an adaptation, the specific characteristics of the different trace gas retrievals and the specific spatial patterns (profiles as well as global distribution) have to be considered in detail. In particular for BrO, the method will be probably insufficient, since the regions of interest for BrO are polar, i.e. SZAs are high, and stratospheric BrO profiles are too low to be fully captured by the limb measurements.

The alternating limb/nadir geometries of SCIAMACHY are not available for other satellite spectrometers like GOME-2 or OMI. Nevertheless, the information on the longitudinal dependency of stratospheric NO_2 CDs, as provided by SCIAMACHY limb measurements, could generally be used to also correct RSM stratospheric estimations of other satellite instruments. However, for such comparisons, differences in local times of the measurements have to be considered.

AMTD
2, 2983–3025, 2009

Acknowledgements. We thank ESA and DLR for providing SCIAMACHY spectra. S. Kühl is funded by the DFG (Deutsche Forschungsgemeinschaft). We gratefully acknowledge valuable discussions with Andreas Richter and Andreas Hilboll.

The service charges for this open access publication have been covered by the Max Planck Society.

References

Beirle, S., Platt, U., Wenig, M., and Wagner, T.: Weekly cycle of NO_2 by GOME measurements: a signature of anthropogenic sources, Atmos. Chem. Phys., 3, 2225–2232, 2003, http://www.atmos-chem-phys.net/3/2225/2003/.

Beirle, S.: Estimating source strengths and lifetime of Nitrogen Oxides from satellite data, PhD Thesis, University of Heidelberg, 2004.

Boersma, K. F., Eskes, H. J., and Brinksma, E. J.: Error analysis for tropospheric NO_2 retrieval from space, J. Geophys. Res., 109, D04311, doi:10.1029/2003JD003962, 2004.

Boersma, K. F., Eskes, H. J., Veefkind, J. P., Brinksma, E. J., van der A, R. J., Sneep, M., van den Oord, G. H. J., Levelt, P. F., Stammes, P., Gleason, J. F., and Bucsela, E. J.: Near-real time retrieval of tropospheric NO2 from OMI, Atmos. Chem. Phys., 7, 2103–2118, 2007, http://www.atmos-chem-phys.net/7/2103/2007/.

Bovensmann, H., Burrows, J. P., Buchwitz, M., Frerick, J., Noël, S., Rozanov, V. V., Chance, K. V., and Goede, A. P. H.: SCIAMACHY: Mission objectives and measurement modes, J. Atmos. Sci., 56(2), 127–150, 1999.

Brühl, C. and Crutzen, P. J.: MPIC two-dimensional model, in: The Atmospheric Effect of Stratospheric Aircraft, 1292, edited by: Prather, M. J. and Remsberg, E. E., NASA Ref. Publications, 103–104, 1993. 2991

Bucsela, E. J., Celarier, E. A., Wenig, M. O., Gleason, J. F., Veefkind, J. P., Boersma, K. F., and Brinksma, E. J.: Algorithm for NO_2 Vertical Column Retrieval from the Ozone Monitoring Instrument, IEEE T. Geosci. Remote, 44(5), 1245–1258, 2006.

Burrows, J., Weber, M., Buchwitz, M., Rozanov, V. V., Ladstädter-Weissenmayer, A., Richter, A., de Beek, R., Hoogen, R., Bramstedt, K., Eichmann, K.-U., Eisinger, M., and Perner,

D.: The Global Ozone Monitoring Experiment (GOME): Mission concept and first scientific results, J. Atmos. Sci., 56, 151–175, 1999.

Butz, A., Bösch, H., Camy-Peyret, C., Chipperfield, M., Dorf, M., Dufour, G., Grunow, K., Jeseck, P., Kühl, S., Payan, S., Pepin, I., Pukite, J., Rozanov, A., von Savigny, C., Sioris, C., Wagner, T., Weidner, F., and Pfeilsticker, K.: Inter-comparison of stratospheric O_3 and NO_2 abundances retrieved from balloon borne direct sun observations and Envisat/SCIAMACHY limb measurements, Atmos. Chem. Phys., 6, 1293–1314, 2006, http://www.atmos-chem-phys.net/6/1293/2006/. 2992

Deutschmann, T.: Atmospheric radiative transfer modelling using Monte Carlo methods, Diploma Thesis, Universität Heidelberg, 2009. 2991

Dorf, M., Bösch, H., Butz, A., Camy-Peyret, C., Chipperfield, M. P., Engel, A., Goutail, F., Grunow, K., Hendrick, F., Hrechanyy, S., Naujokat, B., Pommereau, J.-P., Van Roozendael, M., Sioris, C., Stroh, F., Weidner, F., and Pfeilsticker, K.: Balloon-borne stratospheric BrO measurements: comparison with Envisat/SCIAMACHY BrO limb profiles, Atmos. Chem. Phys., 6, 2483–2501, 2006, http://www.atmos-chem-phys.net/6/2483/2006/. 2992

Fishman, J. and Balok, A. E.: Calculation of daily tropospheric ozone residuals using TOMS and empirically improved SBUV measurements: Application to an ozone pollution episode over the eastern United States, J. Geophys. Res.-Atmos., 104, 30319–30340, 1999.

Franke, K., Richter, A., Bovensmann, H., Eyring, V., Jöckel, P., Hoor, P., and Burrows, J. P.: Ship emitted NO_2 in the Indian Ocean: comparison of model results with satellite data, Atmos. Chem. Phys., 9, 7289–7301, 2009, http://www.atmos-chem-phys.net/9/7289/2009/.

Heckel, A., Richter, A., Rozanov, A., and Burrows, J. P.: Limb Nadir Matching: Retrieval of tropospheric NO_2 columns using SCIAMACHY Nadir and Limb measurements, Presentation at the workshop "Tropospheric NO_2 measured by satellites", 10–12 September 2007, KNMI, De Bilt, The Netherlands, online available at: http://www.knmi.nl/research/climate_observations/events/no2_workshop/presentations/Presentations/107_Heckel.ppt, 2007.

Kühl, S., Pukīte, J., Deutschmann, T., Platt, U., and Wagner, T.: SCIAMACHY Limb Measurements of NO_2, BrO and OClO, Retrieval of vertical profiles: Algorithm, first results, sensitivity and comparison studies, Adv. Space Res., 42, 1747–1764, 2008. 2991, 2992

Leue, C., Wenig, M., Wagner, T., Klimm, O., Platt, U., and Jähne, B.: Quantitative analysis of NO_x Emissions from Global Ozone Monitoring Experiment satellite image sequences, J.

Geophys. Res., 106, 5493–5505, 2001.
Levelt, P. F., van den Oord, G. H. J., Dobber, M. R., Malkki, A., Visser, H., de Vries, J., Stammes, P., Lundell, J. O. V., and Saari, H.: The ozone monitoring instrument, IEEE T. Geosci. Remote, 44(5), 1093–1101, 2006.
Martin, R. V., Chance, K., Jacob, D. J., Kurosu, T. P., Spurr, R. J. D., Bucsela, E., Gleason, J. F., Palmer, P. I., Bey, I., Fiore, A. M., Li, Q., Yantosca, R. M., and Koelemeijer, R. B. A.: An improved retrieval of tropospheric nitrogen dioxide from GOME, J. Geophys. Res., 107(D20), 4437, doi:10.1029/2001JD001027, 2002.
Martin, R. V.: Satellite remote sensing of surface air quality, Atmos. Environ., 42, 7823–7843, 2008.
Menke, W.: Geophysical data analysis: discrete inverse theory, Academic Press, 1999. 2991
Platt, U. and Stutz, J., Differential Optical Absorption Spectroscopy Principles and Applications, Series: Physics of Earth and Space Environments, Springer, ISBN 978-3-540-21193-8, 2008.
Polovina, J. J., Howell, E. A., and Abecassis, M.: Oceans least productive waters are expanding, Geophys. Res. Lett. 35, L03618, doi:10.1029/2007GL031745, 2008.
PROMOTE, PROtocol MOniToring for the GMES Service Element on Atmospheric Composition, online available at: http://www.iup.uni-bremen.de/doas/no2_promote.htm, 2004.
Puķīte, J., Kühl, S., Deutschmann, T., Wilms-Grabe, W., Friedeburg, C., Platt, U., and Wagner, T.: Retrieval of stratospheric trace gases from SCIAMACHY limb measurements, Proceedings of the First Atmospheric Science Conference, 8–12 May, ESA/ESRIN, Frascati, Italy, ESA SP-628, available at: http://earth.esa.int/workshops/atmos2006/participants/1148/paper_proc_Frasc_2.pdf, 2006. 2991, 2992
Puķīte, J., Kühl, S., Deutschmann, T., Platt, U., and Wagner, T.: Accounting for the effect of horizontal gradients in limb measurements of scattered sunlight, Atmos. Chem. Phys., 8, 3045–3060, 2008, http://www.atmos-chem-phys.net/8/3045/2008/.
Puķīte, J., Kühl, S., Deutschmann, T., Platt, U., and Wagner, T.: Extending differential optical absorption spectroscopy for limb measurements in the UV, Atmos. Meas. Tech. Discuss., 2, 2919–2982, 2009a, http://www.atmos-meas-tech-discuss.net/2/2919/2009/. 2992
Puķīte, S. Kühl, T. Deutschmann, U. Platt, and Wagner, T.: Profile retrieval from SCIAMACHY limb measurements by global 2D tomography, in preparation, 2009b.

Richter, A. and Wagner, T.: Diffuser Plate Spectral Structures and their Influence on GOME Slant column densities, Technical Note, online available at: http://joseba.mpch-mainz.mpg.de/pdf_dateien/diffuser_gome.pdf, January 2001.

Richter, A. and Burrows, J. P.: Tropospheric NO_2 from GOME Measurements, Adv. Space Res., 29(11), 1673–1683, 2002.

Richter, A., Burrows, J. P., Nüß, H., Granier, C., and Niemeier, U.: Increase in tropospheric nitrogen dioxide over China observed from space, Nature, 437, 129–132, doi:10.1038/nature04092, 2005.

Sierk, B., Richter, A., Rozanov, A., von Savigny, Ch., Schmoltner, A. M., Buchwitz, M., Bovensmann, H., and Burrows, J. P.: Retrieval and monitoring of atmospheric trace gas concentrations in nadir and limb geometry using the space-borne SCIAMACHY instrument, Environ. Monit. Assess., 120, 65–77, doi:10.1007/s10661-005-9049-9, 2006.

Sioris, C. E., Kurosu, T. P., Martin, R. V., and Chance, K.: Stratospheric and tropospheric NO2 observed by SCIAMACHY: first results Adv. Space Res., 34(4), 780–785, 2004.

Vasilkov, A. P., Joiner, J., Gleason, J., and Bhartia, P.: Ocean Raman scattering in satellite backscatter UV measurements, Geophys. Res. Lett., 29, 1837–1840, 2002.

Vountas, M., Richter, A., Wittrock, F., and Burrows, J. P.: Inelastic scattering in ocean water and its impact on trace gas retrievals from satellite data, Atmos. Chem. Phys., 3, 1365–1375, 2003, http://www.atmos-chem-phys.net/3/1365/2003/.

Wagner, T., Beirle, S., Deutschmann, T., Eigemeier, E., Frankenberg, C., Grzegorski, M., Liu, C., Marbach, T., Platt, U., and Penning de Vries, M.: Monitoring of atmospheric trace gases, clouds, aerosols and surface properties from UV/vis/NIR satellite instruments, J. Opt. A., Pure Appl. Opt., 10, 104019, doi:10.1088/1464-4258/10/10/104019, 2008.

Wenig, M., Kühl, S., Beirle, S., Bucsela, E., Jähne, B., Platt, U., Gleason, J., and Wagner, T.: Retrieval and analysis of stratospheric NO_2 from the Global Ozone Monitoring Experiment, J. Geophys. Res., 109, D04315, doi:10.1029/2003JD003652., 2004.

Ziemke, J. R., Chandra, S., and Bhartia, P. K.: "Cloud slicing": A new technique to derive upper tropospheric ozone from satellite measurements, J. Geophys. Res.-Atmos., 106, 9853–9867, 2001.

Table 1. Abbreviations and Variables used in this study

Symbol	Abbreviation	Quantity
α	SZA	Solar Zenith Angle
β	LZA	Line of sight Zenith Angle
Λ	lat	latitude
Φ	lon	longitude
d		day (time variable)
	CD	Column Density
S	SCD	Slant Column Density
V	VCD	Vertical Column Density
V^*		VCD derived with stratospheric AMF
W		Stratospheric VCD
A	AMF	Air Mass Factor
L	LVCD	Limb Vertical Column Density (integrated profile)
T	TSCD	Tropospheric Slant Column Density
subscript $_{RS}$	RS	(in the) Reference Sector
subscript $_{Strat}$		Stratospheric
	SES	Stratospheric Estimation Scheme
	RSM	SES 1: Reference Sector Method
	ALC	SES 2: Absolute Limb Correction
	RLC	SES 3: Relative Limb Correction
ΔL	LLV	Longitudinal Limb Variation
s	std	Standard deviation
δ		Error
$\widehat{\ }$	LUT	Smoothed and interpolated look up table

AMTD
2, 2983–3025, 2009

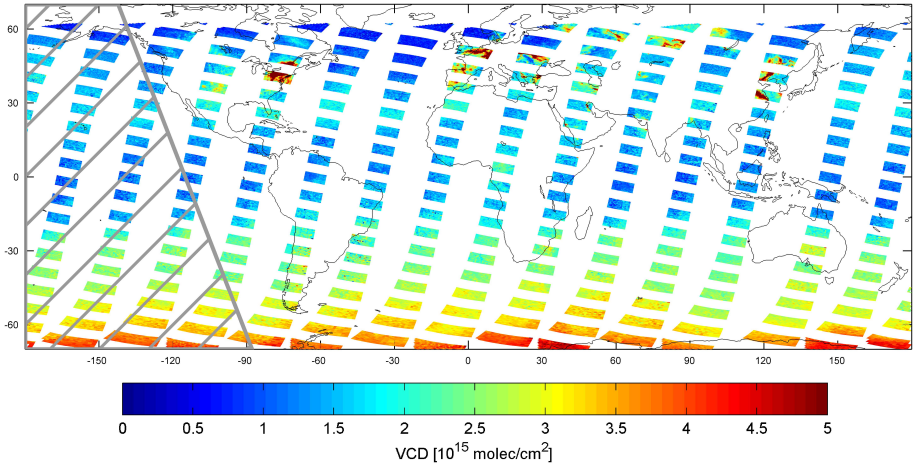

Fig. 1. Nadir VCD V^* for 28 January 2006. The marked area in the Pacific is the reference sector used in this study.

AMTD

2, 2983–3025, 2009

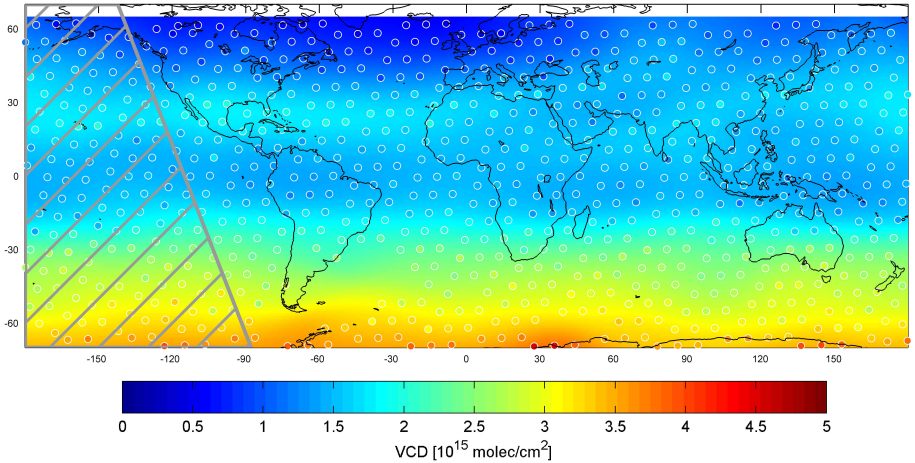

Fig. 2. Stratospheric VCD L derived from integrated limb profiles 27–29 January 2006. Colour-coded disks indicate the location of the tangent points for the individual limb VCDs L, the map shows the interpolated and smoothed field $\widehat{L}(d, \Lambda, \phi)$.

AMTD
2, 2983–3025, 2009

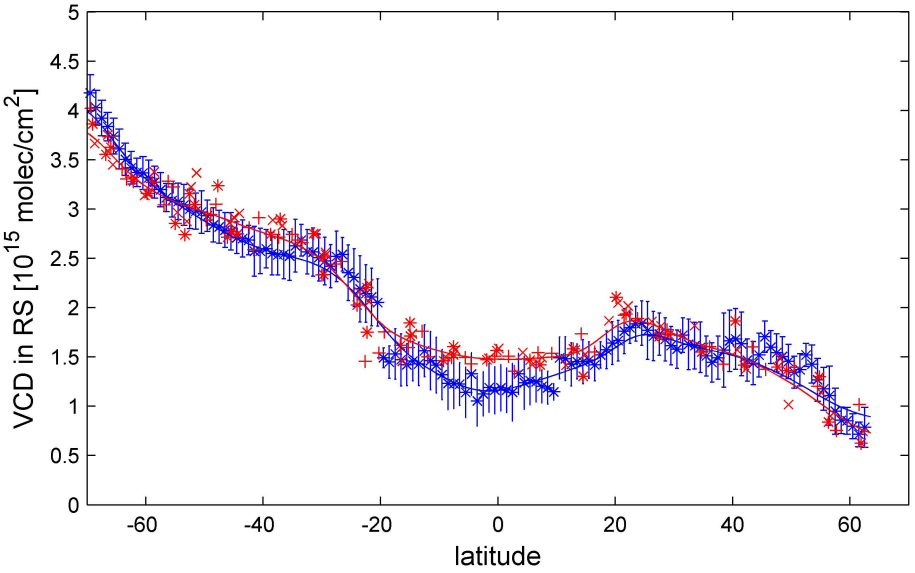

Fig. 3. Latitudinal dependencies of V^*_{RS} (blue) and L_{RS} (red). Nadir measurements are binned in 1° bins and displayed as mean (*) and standard deviation (bar). Limb measurements are displayed for January 27 (+), 28 (*), and 29 (x), 2006. The curves show the smoothed LUTs $\widehat{V}_{RS}(d,\Lambda)$ (blue) and $\widehat{L}_{RS}(d,\Lambda)$ (red).

AMTD
2, 2983–3025, 2009

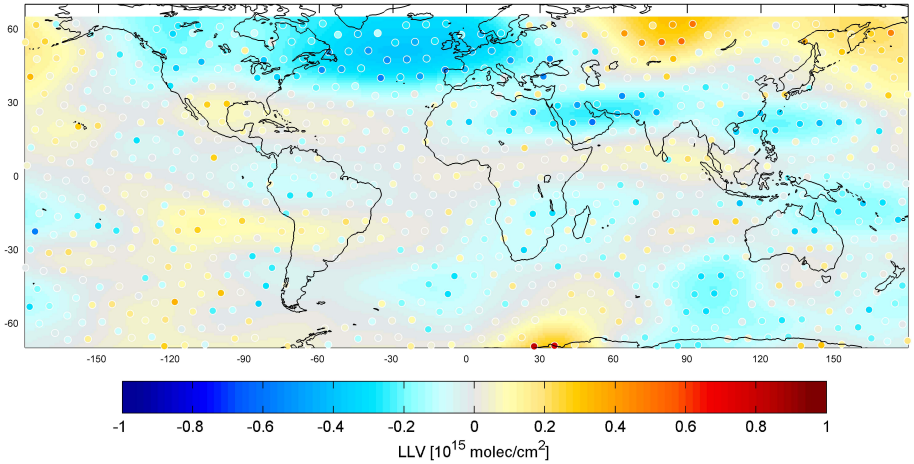

Fig. 4. Longitudinal Limb Variation (LLV) ΔL for 28 January 2006. Disks show the LLV for the individual limb states (ΔL), the map shows the interpolated and smoothed field $\widehat{\Delta L}(d, \Lambda, \Phi)$.

AMTD
2, 2983–3025, 2009

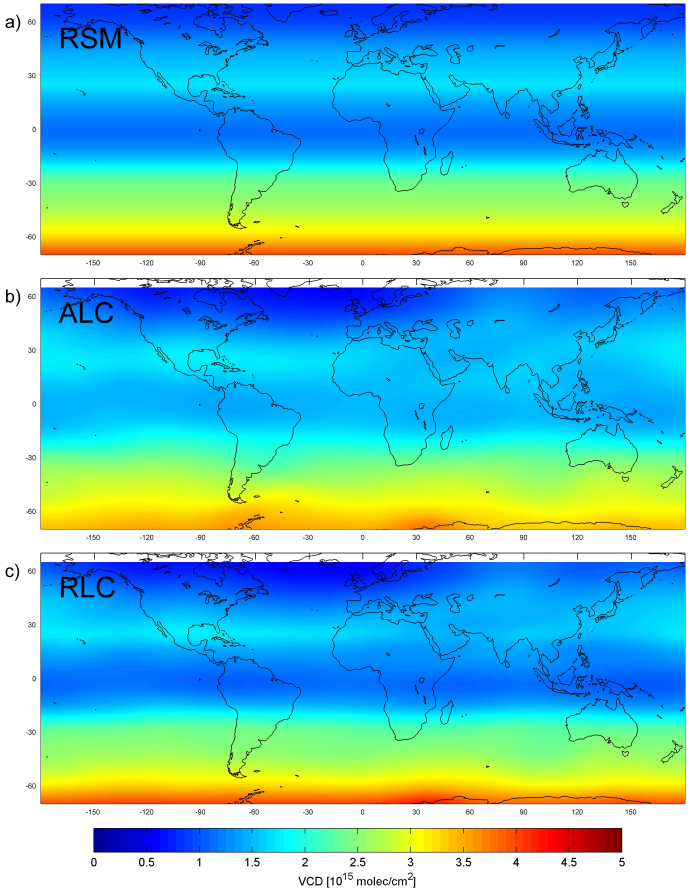

Fig. 5. Stratospheric VCDs *W* on 28 January 2006 for the different stratospheric estimation schemes: (a) Reference Sector Method, **(b)** Absolute Limb Correction, and **(c)** Relative Limb Correction.

AMTD
2, 2983–3025, 2009

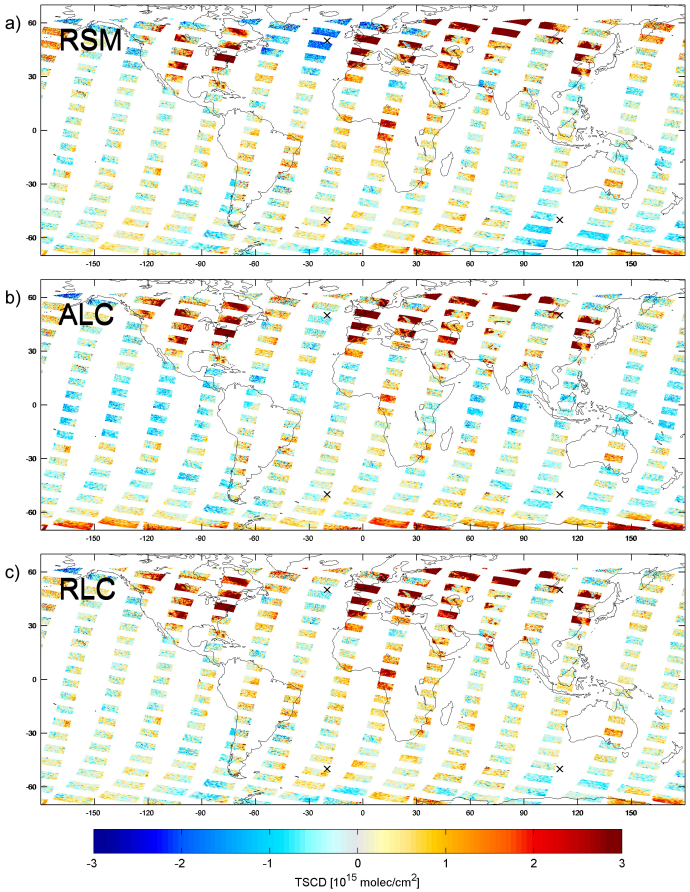

Fig. 6. Tropospheric SCDs for 28 January 2006. **(a)** T_{RSM}: Reference Sector Method. **(b)** T_{ALC}: Absolute Limb Correction. **(c)** T_{RLC}: Relative Limb Correction.

AMTD
2, 2983–3025, 2009

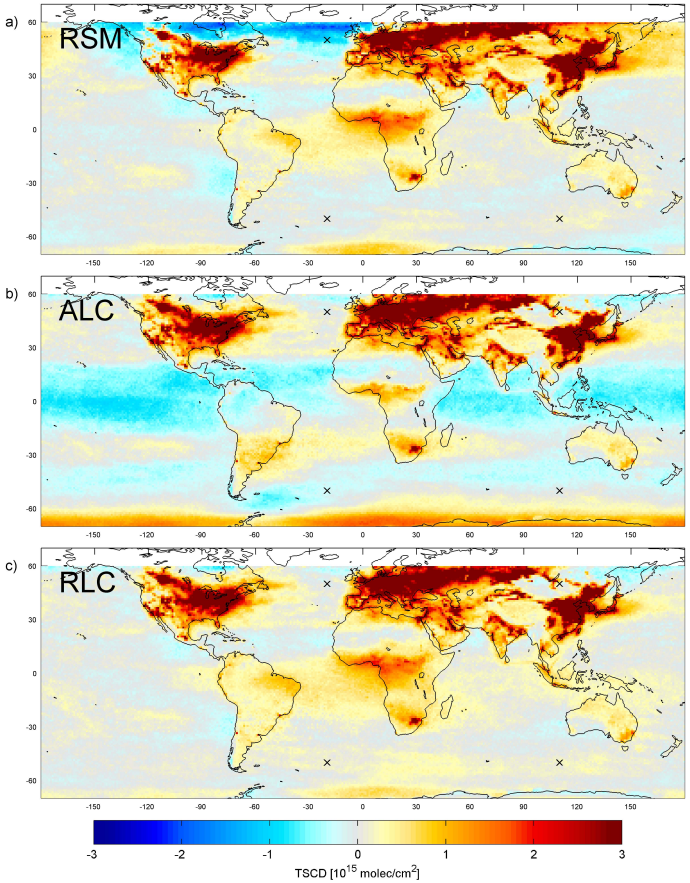

Fig. 7. Mean tropospheric SCDs for January 2003–2008. **(a)** T_{RSM}: Reference Sector Method. **(b)** T_{ALC}: Absolute Limb Correction. **(c)** T_{RLC}: Relative Limb Correction.

AMTD
2, 2983–3025, 2009

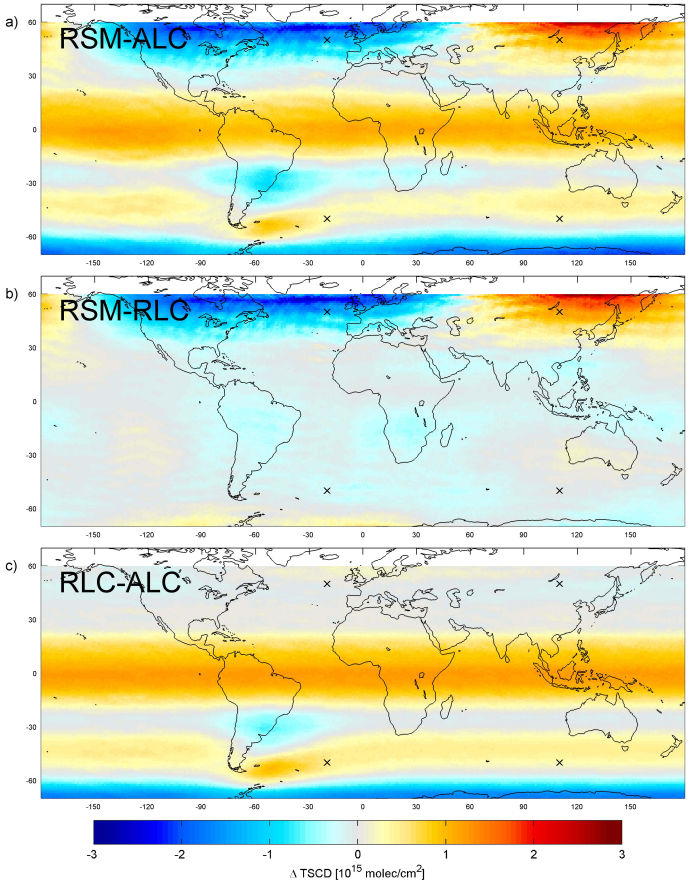

Fig. 8. Difference of mean tropospheric SCDs $T_{RSM} - T_{ALC}$ **(a)**, $T_{RSM} - T_{RLC}$ **(b)**, and $T_{RLC} - T_{ALC}$ **(c)** for January 2003–2008.

AMTD
2, 2983–3025, 2009

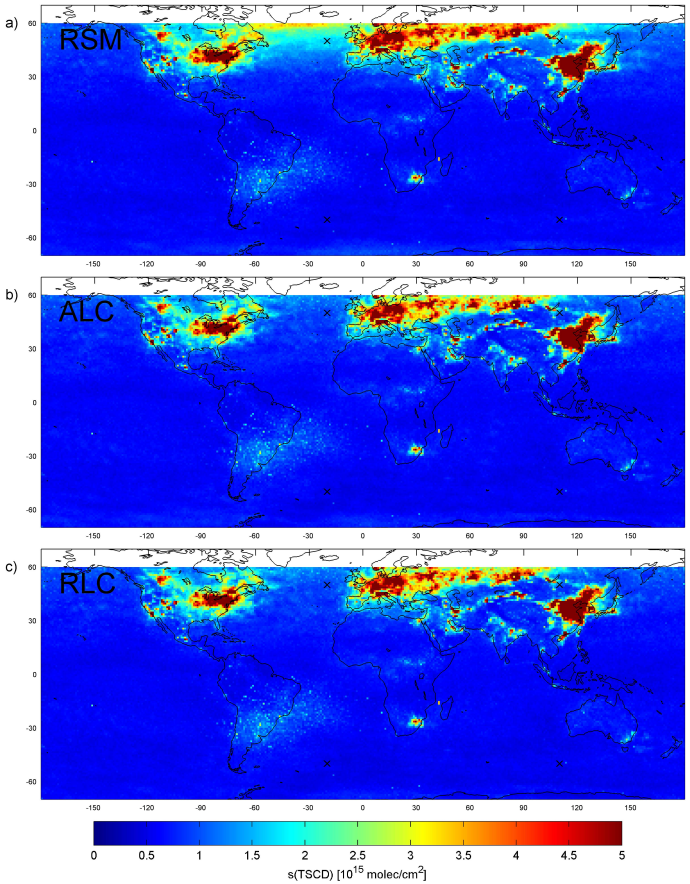

Fig. 9. Standard deviations of tropospheric SCDs for January 2003–2008. **(a)** $s(T_{RSM})$, **(b)** $s(T_{ALC})$, **(c)** $s(T_{RLC})$.

AMTD
2, 2983–3025, 2009

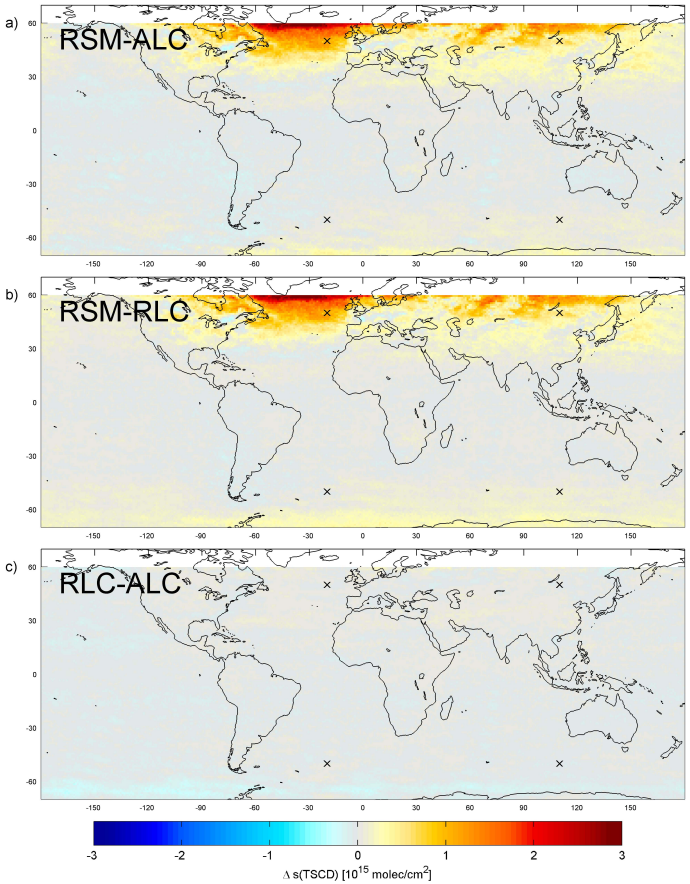

Fig. 10. Difference of the standard deviations of tropospheric SCDs $s(T_{RSM}) - s(T_{ALC})$ **(a)**, $s(T_{RSM}) - s(T_{RLC})$ **(b)**, and $s(T_{RLC}) - s(T_{ALC})$ **(c)** for January 2003–2008.

AMTD
2, 2983–3025, 2009

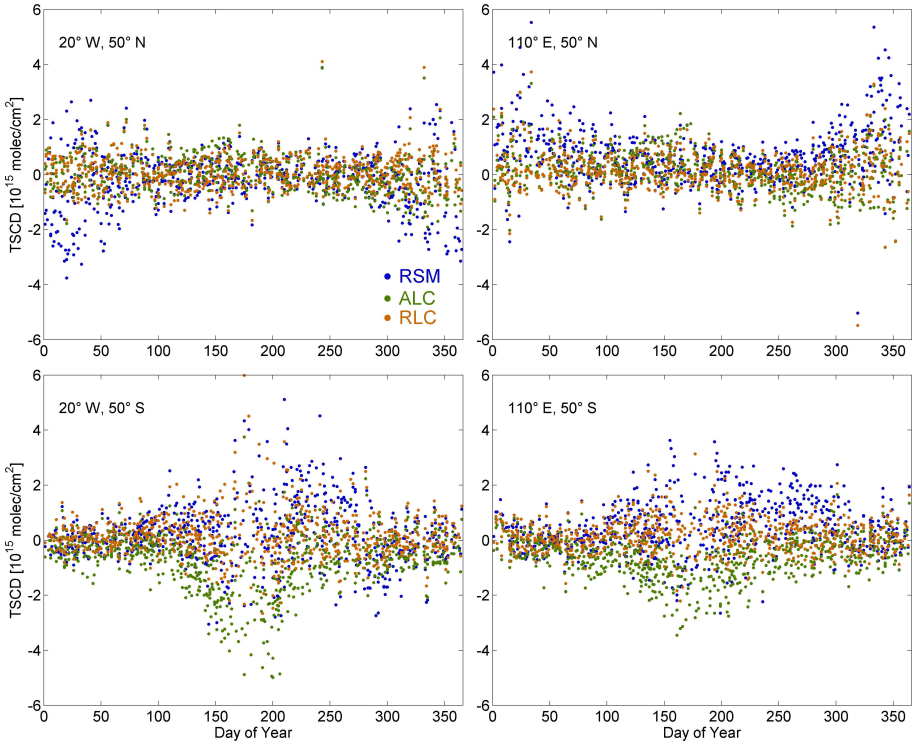

Fig. 11. Annual cycle of TSCDs for four selected locations (as marked in Figs. 6–10). Upper row: 50° N. Lower row: 50° S. Left column: 20° W. Right column: 110° E. The different schemes are marked by colors: blue (T_{RSM}), green (T_{ALC}), and orange (T_{RLC}).

AMTD
2, 2983–3025, 2009

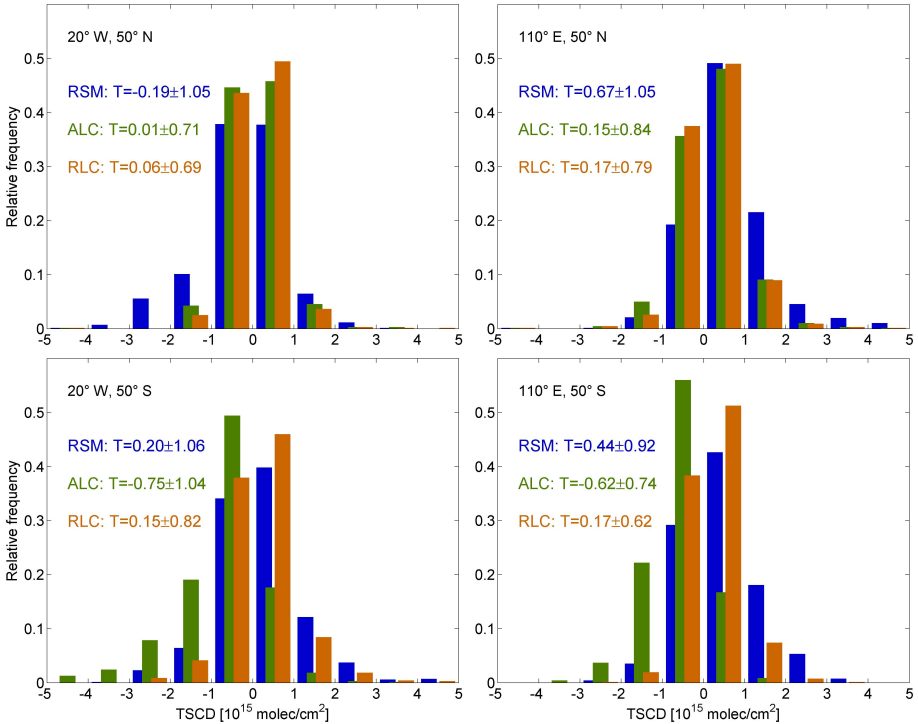

Fig. 12. Frequency distribution of TSCDs for four selected locations (as marked in Figs. 6–10). Upper row: 50° N. Lower row: 50° S. Left column: 20° W. Right column: 110° E. The different schemes are marked by colors: blue (T_{RSM}), green (T_{ALC}), and orange (T_{RLC}). The numbers give the respective means and standard deviations (in 10^{15} molec/cm^2).

AMTD
2, 2983–3025, 2009